Separation Science and Technology
Publication details, including instructions for authors and subscription information:
http://www.informaworld.com/smpp/title~content=t713708471

Application of Modified Water Nut Carbon as a Sorbent in Congo Red and Malachite Green Dye Contaminated Wastewater Remediation

Rais Ahmad[a]; Pijush Kanti Mondal[a]
[a] Environmental Research Laboratory, Department of Applied Chemistry, Faculty of Engineering and Technology, Aligarh Muslim University, Aligarh, UP, India

To cite this Article Ahmad, Rais and Mondal, Pijush Kanti(2010) 'Application of Modified Water Nut Carbon as a Sorbent in Congo Red and Malachite Green Dye Contaminated Wastewater Remediation', Separation Science and Technology, 45: 3, 394 — 403

To link to this Article: DOI: 10.1080/01496390903484875

URL: http://dx.doi.org/10.1080/01496390903484875

Separation Science and Technology, 45: 394–403, 2010

ISSN: 0149-6395 print/1520-5754 online
DOI: 10.1080/01496390903484875

Application of Modified Water Nut Carbon as a Sorbent in Congo Red and Malachite Green Dye Contaminated Wastewater Remediation

Rais Ahmad and Pijush Kanti Mondal
Environmental Research Laboratory, Department of Applied Chemistry, Faculty of Engineering and Technology, Aligarh Muslim University, Aligarh, UP, India

Batch and column adsorption experiments were conducted to investigate the removal of dyes from wastewater by water nut modified carbon (WNMC). Acidic pH was favorable for adsorption for Congo red dyes and basic pH was favorable for the adsorption for Malachite green dyes. The surface property of the sorbent was characterized by scanning electron microscopy and Fourier transform infrared techniques. The adsorption process was found to be endothermic and spontaneous. Different models of adsorption were used to describe the kinetics data and to calculate the corresponding rate constants of WNMC surfaces for dyes adsorption. A mechanism of dyes adsorption associating chemisorption processes is presented allowing the discussion of the variations in adsorption behavior of the material. These data suggested that WNMC are promising materials for dyes sorption. The data were in good agreement with bed depth service time model.

Keywords BDST; breakthrough capacity; characterization; fixed bed column; kinetics; WNMC

INTRODUCTION

Among the different pollutants of aquatic ecosystems, dyes and their derivatives are considered as priority pollutants since they are harmful to organisms even at ppb levels (1). Colored compounds comprising pigments and dyes are used widely in textile, plastic, food, dyeing, paper, printing, pharmaceutical, and cosmetic industries. Textile processing industries nowadays are widespread sectors in developing countries. Among the various processes in the textile industry, the dyeing process uses large volume of water for dyeing, fixing, and washing processes. Thus, the wastewater generated from the textile processing industries contains suspended solids, high amount of dissolved solids, un-reacted dyestuffs (color), and other auxiliary chemicals that are used in the various stages of dyeing and processing. These dyes color the water and make penetration of sunlight to the lower layers impossible and hence affecting aquatic life.

In recent years, several physico-chemical treatments have been proposed for efficient dyes removal, such as adsorption (2,3), advanced oxidation (4,5), heterogeneous photo catalysis (6,7), and biological treatments (8,9). A great variety of adsorbents (natural or synthetic) have been evaluated for the removal of organic substances from aqueous solutions, most of them presenting some limitations such as poor retention capacity or high preparation cost. Nowadays modified carbons are considered as the most effective organics sorbents with high surface areas (10–12). The aim of this study is to evaluate selected WNMC with different physico-chemical characteristics for dye sorption and to understand the corresponding kinetics and adsorption mechanisms. In view of future applications, the regeneration of the most efficient WNMC after adsorption dyes is also reported and discussed.

In India, water nut shells (WNS) litter around streets especially in the eastern areas and they constitute environmental nuisance. It is anticipated that this work would be about the environmental nuisance if the water nut shell are been processed into granulated water nut modified carbon (WNMC) for the removal of different contaminants likely to be encountered in dye containing industrial wastewaters. Hence, agricultural wastes such as water nut shell could be important for the removal of dyes in wastewater. Thus, the potential for using agricultural waste (WNS) that litter our environment may be valuable resources for the removal of organic matter from industrial wastewater.

MATERIALS AND METHODS

Preparation of Modified Carbon from Water Nut Shell

Water nuts shells, an agricultural waste, was washed, crushed, and finally ground in a laboratory mill to a size of 100–150 mesh (BSS standard) particles size and afterwards dried in an air oven at 105°C. In this experiment the carbonization step was held for 2 hr at 500°C. This temperature to be an optimum with many agricultural raw materials

---

Received 20 April 2009; accepted 29 October 2009.

Address correspondence to Rais Ahmad, Environmental Research Laboratory, Department of Applied Chemistry, Faculty of Engineering and Technology, Aligarh Muslim University, Aligarh, UP 202 002, India. E-mail: raisdye@gmail.com

(13–16). Introduced in a tube furnace and heated slowly to 500°C where it stayed for 2 h. The precursor was thermally decomposed to porous carbonaceous material. The produced carbonized material was washed thoroughly with hot water and dried till constant weight. The water nut modified carbon was dried overnight in an oven at 110°C, cooled at room temperature, and stored in desiccators until use.

Preparation of H_3PO_4-Treated Modified Carbon

Acid treatment on the water nut shell-based activated carbon was performed by immersing 5 g of the original activated carbon in 100 ml of 5% phosphoric acid (H_3PO_4) and left for 4 h. The sample was then filtered using Whatman No. 1 filter paper to separate the modified carbon from the solution. The modified carbon was then rinsed with deionized water and dried in an oven overnight at 105°C. The chemically treated modified carbon was stored in desiccators to prevent moisture build up.

Dyes and Chemicals

Malachite green (MG) [4-[(4-dimethylaminophenyl)-phenyl-methyl]-N,N-dimethyl-aniline], a cationic triphenylmethane dye used worldwide as a fungicide and antiseptic in the aquaculture industry was a G.R. Product of CDH, India and was used as received. Congo red (CR) [1-naphthalenesulfonic acid, 3,30-(4,40-biphenylenebis (azo)) bis (4-amino-) disodium salt] is a benzidine-based dye was also a G.R. product of CDH, India and was used as received. The dye is known to metabolize to benzidine, a known human carcinogen. Exposure to the dye has been known to cause an allergic reaction. The substance is considered as toxic. All chemicals used were of analytical reagent grade and supplied by CDH India.

Batch Adsorption Studies

The adsorption was performed by batch as well as column experiments. Adsorption experiments were carried out by agitating the adsorbent in 50 ml of dye solution of desired concentration (10 ppm) and 10 mg of weighted adsorbent at room temperature (30 ± 5°C) in a rotary shaker at 200 rpm. The samples were withdrawn from the shaker at predetermined time intervals, and the color of the supernatant solution measured spectrophotometrically using a UV-Visible Spectrophotometer (Elico, Sl-164). The wavelengths 497, 618 nm were used as the monitoring wavelengths for congo red, malachite green respectively. The effect of pH was studied by adjusting the pH of dye solutions using dilute HC1 and NaOH solutions. All experiments were carried out in triplicate with respect to each condition and mean values were presented.

Kinetic Study

The kinetic study was accomplished with suspensions of WNMC (10 mg) in 50 mL of dye solutions (10 ppm). The mixtures were stirred during different time intervals, ranging from 5 to 210 min and then centrifuged. The dye concentrations in supernatants were determined spectrophotometrically using a UV-Visible Spectrophotometer (Elico, Sl-164) at 497, 618 nm wavelength. The sorbed amounts were determined from the difference between the initial and final concentrations.

Sorption Isotherms

The sorption isotherms were established using WNMC suspensions in CR and MG solution at pH 6 and 8, respectively. The solid/solution ratio was 10 mg/50 ml for dye solutions. The temperatures in the experiment ranged from 20, 30, and 40°C respectively. The suspensions were stirred for 210 min and subsequently centrifuged. The equilibrium concentrations of CR and MG in the supernatants were analyzed as mentioned above in the kinetic section.

Fixed Bed Adsorption (Column Study)

For this purpose a mini-column was employed. The capacity of WNMC towards Malachite green and Congo red dye sorption were found to be better than the other adsorbents, and therefore it was of interest to examine the performance of these sorbents in a column system. Column studies were conducted using the down flow technique in which 1 gm of adsorbent was suspended in distilled water for about 15 min and then transferred into four glass columns (1 cm i.d., 25 cm column length) and the glass wool was kept at the bottom of the column to avoid loss of adsorbent with the liquid flow. The dye solution was fed into the column at the flow rate of 1 ml/minute to determine exhaustive capacity. The initial amount of dye in 50 ml feed minus the amount found in the effluent gave the amount of dye retained by the adsorbent. The process was continued until the amount of dye was same as in the 50 ml feed & effluent. Breakthrough curves were constructed as C_t/C_i vs. treated volume.

The Bed Depth Service Time Model (BDST)

A modified form of the equation that expresses the service time at breakthrough, t, as a fixed function of operation parameters is the BDST model (17–19)

$$t = \frac{N_0}{C_0 \nu} Z - \frac{1}{K_a C_o} \ln\left\{\frac{C_0}{C_t} - 1\right\} \tag{1}$$

where C_0 is the initial dye concentration (mg l^{-1}); C_t is the breakthrough dye concentration (mg l^{-1}); N_0 is the sorption capacity of bed (mg l^{-1}); υ is the linear velocity (cm h^{-1}), and K_a is the rate constant (l mg^{-1} h^{-1}). A plot of t vs. bed depth, Z, should yield a straight line where N_0 and K; are the adsorption capacity and rate constant, respectively, which can be evaluated. It should be borne in mind that the data used in constructing the BDST model

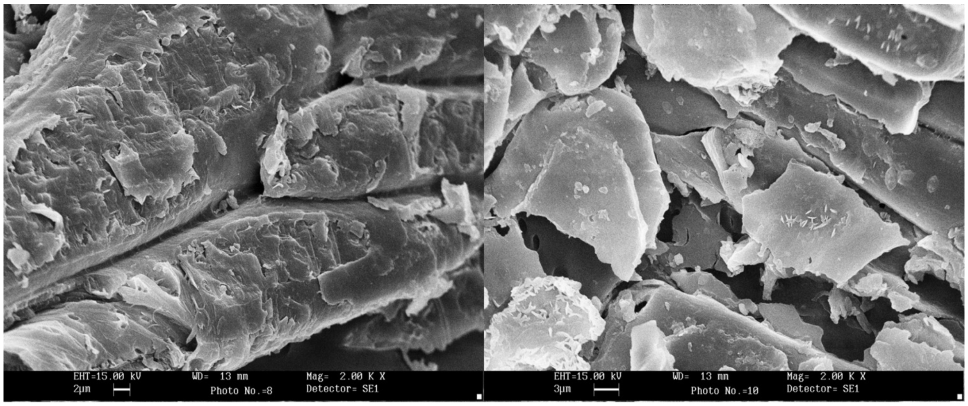

(a) (b)

FIG. 1. Scanning electron micrograph of the adsorbent (a) before carbonification; (b) After carbonification [Magnifications 2000 times].

herein, were obtained using synthetic solutions instead of industrial effluents. The industrial dye effluents usually contain a variety of impurities. These impurities in the effluents could interfere with the sorption of dyes and consequently result in an inaccurate prediction in the treatment of industrial effluents.

RESULTS AND DISCUSSION

Characteristics of Adsorbents

SEM images of carbonified water nut shell are presented here in Fig. 1. It is quite obvious from the obtained SEM images that chemical modification and carbonification adsorbent significantly alters the physico-chemical properties and porosity of the materials. Adsorbents were found to have greater surface area followed by activation. Carbonification is responsible for providing the protons upon ionization in aqueous solutions which in turn can further open the pores of WNS which increases the surface area of the adsorbents.

The FTIR spectra of the inactivated water nut shell displayed the following bands Fig. 2. 3400 cm^{-1} (O–H stretching vibrations), 2250–2400 cm^{-1}(alkyl nitrate), 1559 cm^{-1} (C=C stretching vibration in aromatic rings), and 1086 cm^{-1} (C–OH stretching vibrations). After activation and treated with H_3PO_4, the surface chemistry of the modified carbon underwent some changes and the bands displayed by the FTIR spectra were: 2250–2400 cm^{-1} only withstand, represents alkyl nitrate (cis + trans) mixed bending vibration stretching which signifies their major involvement in the dyes binding behavior.

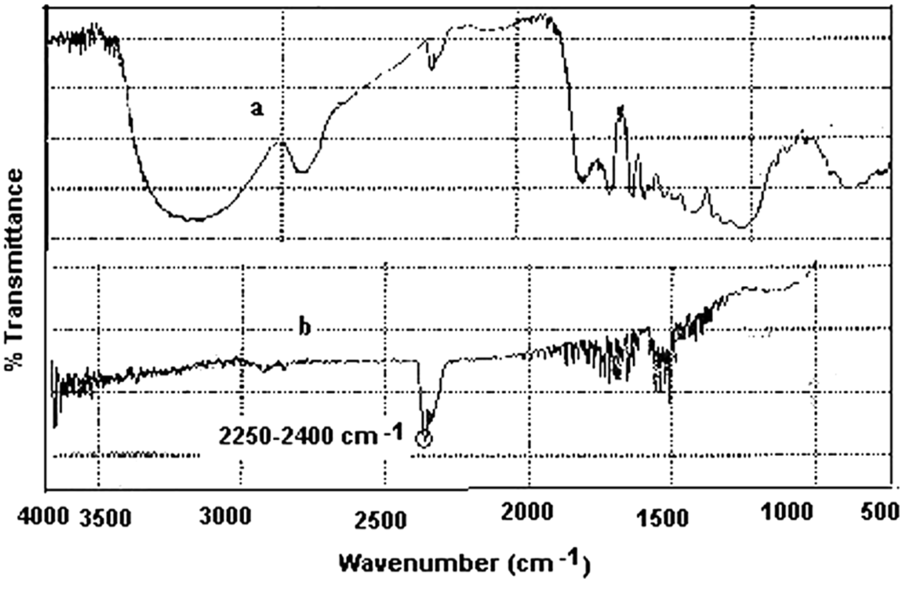

FIG. 2. FTIR spectra of (a) Water nut before carbonification; (b) Water nut after carbonification.

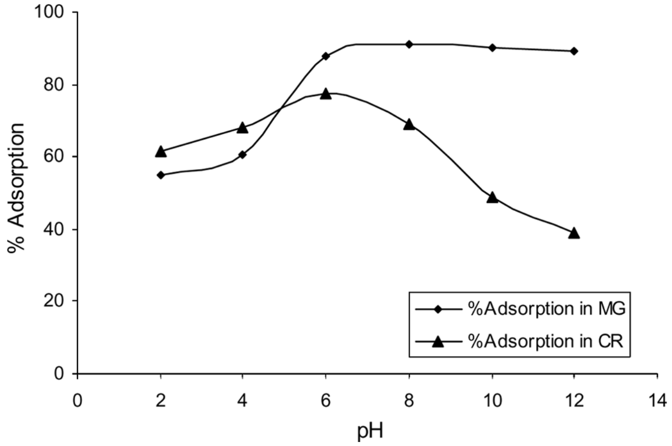

FIG. 3. Effect of pH (Temperature – 30 ± 5°C, pH – 2 to 12, solid ratio – 10 mg WNMC/50 ml dye, initial dye concentration – 10 mg^{-1}).

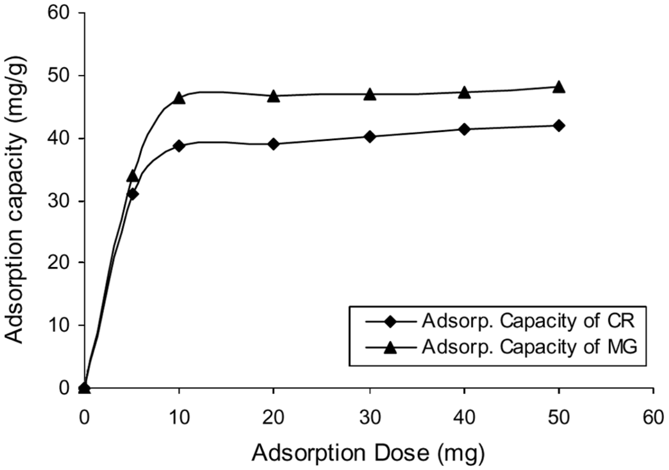

FIG. 4. Effect of adsorption dose (Temperature – 30 ± 5°C, solid ratio – 5 to 50 mg WNMC/50 ml dye, initial dye concentration – 10 mg^{-1}).

Effect of pH

It was observed that the MG and CR removal were highly dependent on the pH of the solution which affected the surface charge of the WNMC (Fig. 3). The results of the experiment done at different pH values, which were conducted to determine the optimum pH range for dye adsorption by WNMC. The percentage removal of Congo red was highest (77.6%) at pH 6.0 and decreased to 39% at pH 12. The percentage removal of Malachite green was highest (91.2%) at pH 8.0. All the experiments were conducted at pH 8.

Effect of Adsorbent Doses

The adsorption capacity (mg/g) of MG and CR by varying the dose of WNMC at 30°C temperature is shown in Fig. 4. The adsorption capacity increases as the adsorbent dose of WNMC is increased. The increase in adsorption density may be due to the fact that some adsorption sites may remain unsaturated during the adsorption process whereas the number of sites available for adsorption increases by increasing the adsorbent doses.

Table 1 lists the comparison of maximum adsorption capacity of dyes on various activated carbons. Although the adsorption capacity of WNMC for dyes was lower than that of oil palm fiber based bamboo dust-based activated carbon, but it was much better than that of other potential adsorbents. According to the results obtained, WNMC was a promising starting material for the preparation of modified carbon for the removal of dyes from aqueous solutions.

Adsorption Kinetics

In order to study the rate determining step for the adsorption of dyes onto the surface of WNMC, the following kinetic models were employed; pseudo-first-order (21), pseudo-second order (22–24), and the intraparticle diffusion. The simple Lagergren pseudo-first-order model assumes that the rate of change of solute uptake with time was directly proportional to the difference in the amount of solute adsorbed at the time of equilibrium q_e [mg/g], and the amount of solute adsorbed at any time, q(t) [mg/g]

$$\frac{dq(t)}{dt} = K_1[q_e - q(t)] \tag{2}$$

where K_1 [1/min] was the rate constant of pseudo-first-order model. When integrating over time and linearizing the model, the following equation was obtained

$$\ln q_e - q(t) = \ln q_e - K_1 t \tag{3}$$

where q_t (mg/g) was the amount of the dye adsorbed at various time, q_{e1} was the maximum adsorption capacity,

TABLE 1
Comparison of the adsorption of dyes on various activated carbons and water nut modified carbon

Adsorbents	Maximum adsorption capacity (mg/g)	References
Water nut modified carbon	46.27 (MG) 38.8 (CR)	This work
Jute fiber–based	136.6 (MB)	(20)
Bamboo dust-based	143.20 (MB)	(20)
Arunda donax root carbon	8.69 (MG)	(20)
Groundnut shell-based	164.90 (MB)	(20)
Oil palm fiber-based	277.8 (MB)	(20)
Activated charcoal	0.180 (MG)	(20)

(MB)-Methylene blue.
(MG)-Malachite Green.
(CR)-Congo Red.

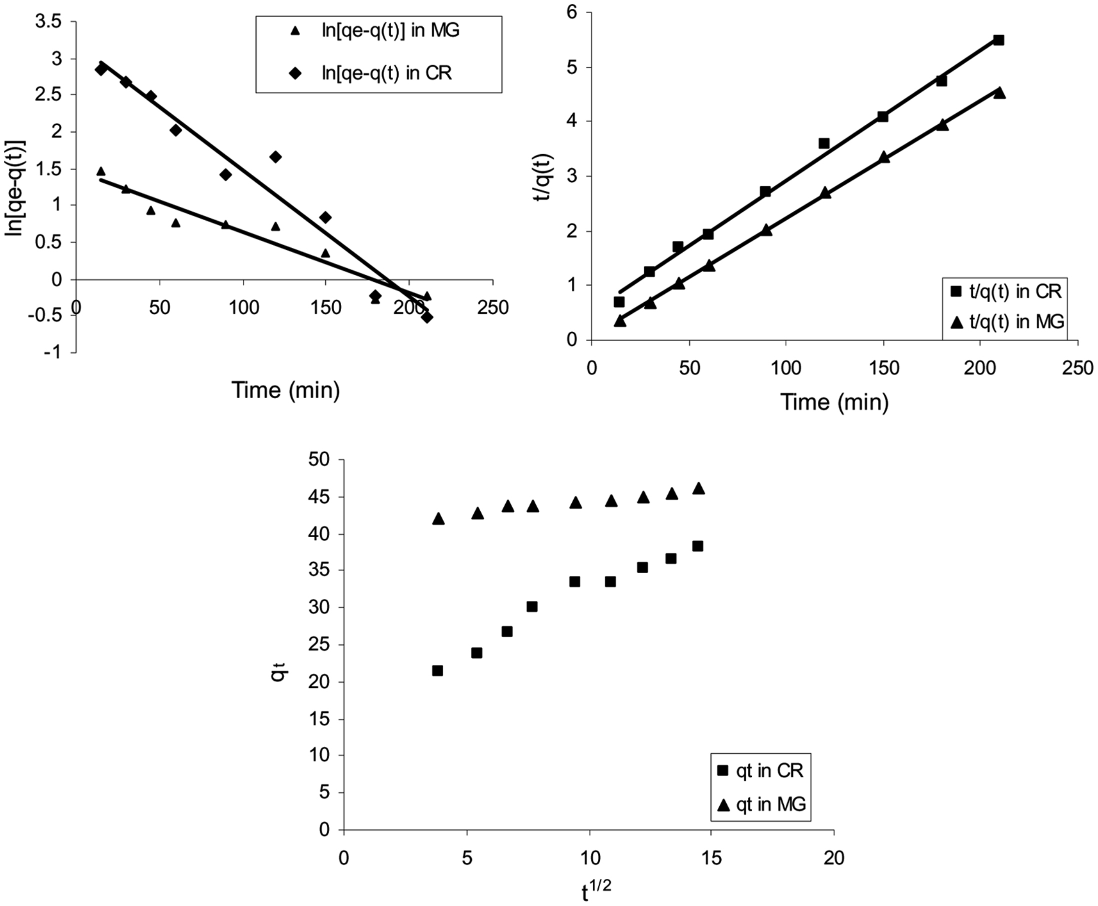

FIG. 5. Representations of the kinetic data by the pseudo first order model, pseudo second-order model and intraparticle diffusion (Temperature – 30 ± 5°C, solid ratio – 0.01 g WNMC/50 ml dye, initial dye concentration – 10 mg^{-1}).

and K_1 (1/min) was the rate constant. Values of K_1 and q_{e1} constants were calculated from the slope and intercept of the plots of $\ln[q_e - q(t)]$ versus t shown in Fig. 5. and were given in Table 2.The pseudo-second-order equation (25) based on the adsorption equilibrium capacity was expressed in Eq. (4).

TABLE 2
Kinetic parameters on the adsorption of MG and CR onto WNMC

	Malachite green	Congo red
Pseudo-first-order equation		
q_e (mg/g)	44.51	32.3
K_1 ($\times 10^2 \text{min}^{-1}$)	0.0083	0.0173
R^2	0.9229	0.9559
Pseudo-second-order equation		
q_e (mg/g)	46.27	38.8
K_2 (g/mg min)	0.0216	0.0277
R^2	0.995	0.9958
Intraparticle diffusion equation		
K_{int} (mg/g min$^{1/2}$)	0.3445	1.558
C	40.943	16.414
R^2	0.9575	0.9622

$$\frac{dq(t)}{dt} = K_2[q_{e2} - q(t)]^2 \tag{4}$$

where K_2 [g/mg/min] was the rate constant of the pseudo-second-order model. When integrating over time and linearizing the model, the following equation was obtained

$$\frac{t}{q_t} = \frac{1}{K_2 q_{e2}^2} + \frac{t}{q_{e2}} \tag{5}$$

where K_2 (g/mg min) was the rate constant and q_{e2} (mg/g) was the maximum adsorption capacity. The second-order constants (K_2 and q_{e2}) were calculated from the slopes and intercepts of Fig. 5.

The rate parameter for intraparticle diffusion was determined using the following equation (26)

$$q_t = K_{int} t^{\frac{1}{2}} + C \tag{6}$$

where C was the intercept and K_{int} was the intraparticle diffusion rate constant (mg/g min$^{-1/2}$). The plot may present multilinearity, indicating that three steps take place. Figure 5 shows the first, sharper portion was attributed to the diffusion of adsorbate through the solution to the external surface of adsorbent or the boundary layer diffusion of solute molecules. The second portion describes the gradual adsorption stage, where intraparticle diffusion was the rate limiting step (27). and the third portion was attributed to the final equilibrium stage.

The correlation coefficients (R^2) and estimated Parameters of described kinetics is given in Table 2. From these values the pseudo-second-order model provided better correlation than the other. While the correlation coefficients for MG and CR were 0.996 and 1 respectively. These figures reflect that the pseudo-second-order model (28) has a better fit with kinetic data. The removal of dyes by adsorption on various materials was found to be rapid at the initial period of contact time and then became slow and stagnant with the increase in contact time. The mechanism for the removal of dyes by adsorption was assumed to involve the following four steps (29).

Overall, the sorption process can be described as follows. Dyes are first adsorbed on the adsorbent surface where some chemical interactions arise. The first step depends not only on the material porosity but also on the availability of the adsorbent that is related to the chemical nature of the surface. Therefore, chemisorptions process occurs when the alkyl nitrate group of the adsorbent interacts with the dye molecule. In the last intraparticle diffusion of dye occurs through the interior pores of the adsorbent particle.

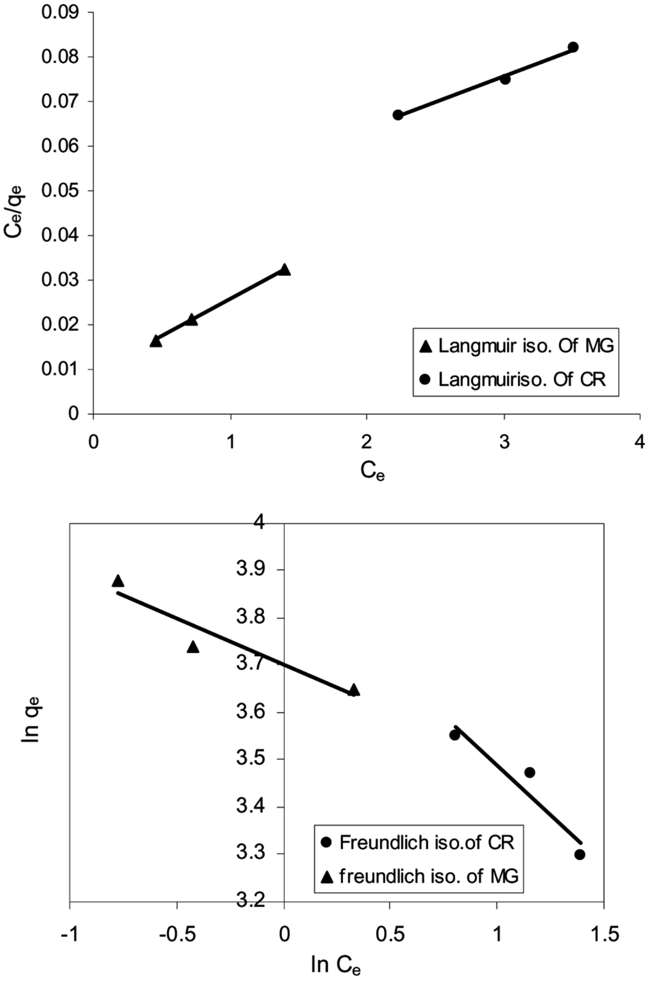

FIG. 6. Isotherm model of MG and CV Dye on WNMC (Temperature – 20, 30, and 40° C, solid ratio – 10 mg WNMC/50 ml dye, initial dye concentration – 10 mg^{-1}).

Adsorption Isotherms

The Langmuir isotherm (30) is based on an assumption that the adsorption occurs at specific homogeneous sites within the adsorbent and the monolayer adsorption onto a surface containing a finite number of adsorption sites of uniform strategies of adsorption with no transmigration of adsorbate in the plane of the surface. The linear form of the Langmuir isotherm equation is given as:

$$\frac{C_e}{q_e} = \frac{1}{Q_0 b} + \frac{1}{Q_0} C_e \tag{4}$$

where C_e is the equilibrium concentration of adsorbate (mg/l); q_e the adsorption capacity (mg/g); and b and q_m are the Langmuir constants. The values of Langmuir constants b and q_m were calculated from the slope and intercept of the linear plot of C_e/q_e versus C_e (Fig. 6). The coefficient b in the Langmuir equation is a measure of the stability of the complex formed between the dye and the adsorbent under specified experimental conditions.

The essential feature of the Langmuir isotherm can be expressed in terms of dimensionless constant separation or equilibrium parameter (R_L), which is defined as:

$$R_L = \frac{1}{1 + bC_0} \tag{5}$$

where, C_0 is the initial dye concentration (mg/l) and b is the Langmuir constant. The value of R_L calculated from different initial concentrations is reported in Table 2. The value of R_L indicates the type of the isotherm to be either unfavorable ($R_L > 1$), linear ($R_L = 1$), favorable ($0 < R_L < 1$), or irreversible ($R_L = 0$) (31). The R_L for MG is 0.65 and The R_L for CR is 0.53. The values are in between 0 and 1 showing favorable adsorption on WNAC.

The Freundlich isotherm on the other hand assumes heterogeneous surface energies in which the energy term in the Langmuir equation varies as a function of the surface coverage (31). The well known linear form of the Freundlich isotherm (32) is given by the following equation:

$$\ln q_e = \ln K_f + \frac{1}{n} \ln C_e \tag{6}$$

where C_e is the equilibrium concentration of the adsorbate (mg/l), q_e is the amount of adsorbate adsorbed per unit mass of adsorbent (mg/g), and K_f and n are Freundlich constants with n giving an indication of how favorable the adsorption process. K_f (mg/g) is the adsorption capacity of the adsorbent which can be defined as the adsorption or distribution coefficient and represents the quantity of dye adsorbed onto WNMC for a unit equilibrium concentration. The slope of 1/n ranging between 0 and 1 is a measure of adsorption intensity or surface heterogeneity, becoming more heterogeneous as its value gets closer to zero (33). A value for 1/n below one indicates a normal Langmuir isotherm. While 1/n above one is indicative of cooperative adsorption (34). The plot of log q_e versus log C_e (Fig. 7) gave a straight line with the slope of 1/n whereas K_f was calculated from the intercept value.

Table 3 summarizes all the constants, correlation coefficients, and R^2 values obtained for the two isotherm models for adsorption of CR and MG on the WNMC. The Langmuir model yielded the best fit, as the R^2 values were relatively high close to unity.

Effect of Temperature

The temperature dependence of adsorption process was a complex phenomenon. The effect of temperature on adsorption of MG and CR on the WNMC were investigated by varying the adsorption temperature at 20, 30, and 40°C (35). The adsorption of MG on the WNAC was found to gradually increase when the temperature was increased from 20 to 40°C for (10 mg/l) concentrations studied. In case of CR the % adsorption was drastically changed when the temperature was increased from 20 to 40°C.

When the temperature increases, the percentage of dye removal increased. The change in standard free energy (ΔG^0), enthalpy (ΔH^0) and entropy (ΔS^0) of adsorption were calculated from the following equation:

$$\Delta G = -RT \ln K_c \tag{7}$$

where R was the gas constant, K_c the equilibrium constant, and T was the temperature in K. The K_c value was calculated from Eq. (7):

$$K_c = \frac{C_{Ae}}{C_{Se}} \tag{8}$$

where C_{Ae} and C_{Se} were the equilibrium concentration of dye ions on adsorbent (mg/L) and in the solution (mg/L), respectively. Standard enthalpy (ΔH^0) and entropy (ΔS^0) of adsorption can be estimated from the van't Hoff equation given in

$$\ln K_c = \frac{\Delta H^0_{ads}}{RT} + \frac{\Delta S^0}{R} \tag{9}$$

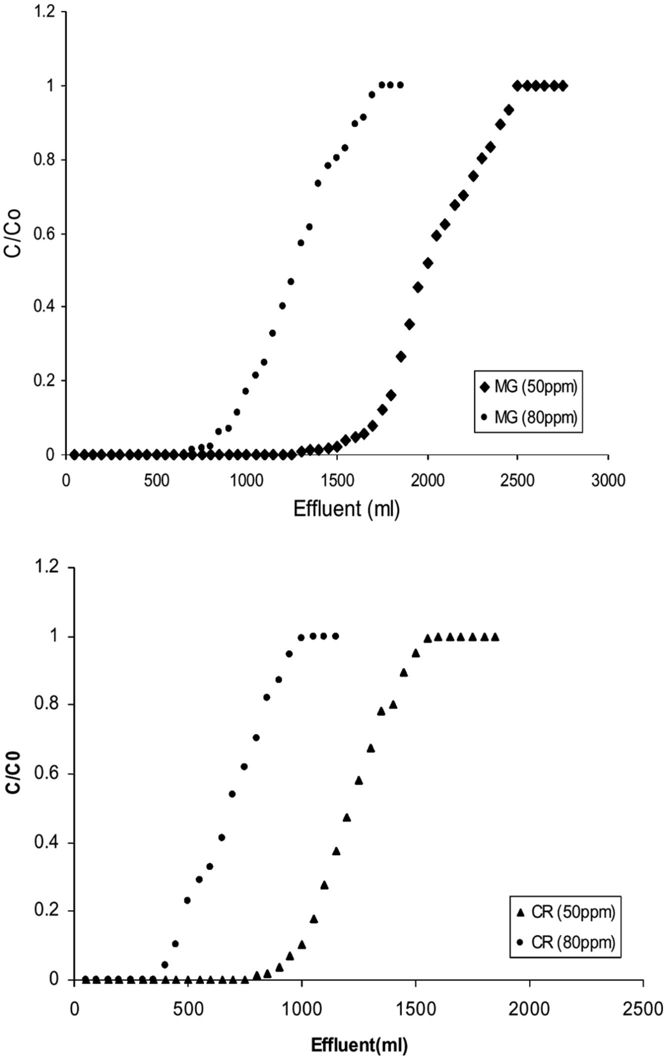

FIG. 7. Break through capacity of MG and CR, Condition: Flow rate = 1 ml/min, temp. – 30 ± 5°C, dose = 1 g, conc. = 50 mg^{-1}, 80 mg^{-1}. (Dia.1 cm).

TABLE 3
Langmuir and Freundlich constant for this adsorption

	Langmuir constant				Freundlich constant		
Dye	q_m (mg/g)	b (l/mg)	R^2	R_L	K_f (mg/g)	n	R^2
MG	47.69	0.053	0.9984	0.65	43.65	−5.14	0.876
CR	38.8	0.088	0.98	0.53	35.45	−2.40	0.897

TABLE 4
Thermodynamic parameters for adsorption

	K_c		ΔG^0 (kj mol^{-1})		ΔH^o (kj mol^{-1})		ΔS^o (kj mol^{-1})	
Temp. (°C)	MG	CR	MG	CR	MG	CR	MG	CR
20°C	6.16	1.09	−4.582	−0.231	48.97	42.19	0.1766	0.1403
30°C	11.25	2.172	−6.297	−2.016	48.97	42.19	0.1766	0.1403
40°C	20.64	3.095	−8.128	−3.031	48.97	42.19	0.1766	0.1403

The slope and intercept of the van't Hoff plot was equal to ΔH^0 ads/R and $\Delta S^0/R$, respectively (36). The thermodynamic parameters obtained are summarized in Table 4. The data obtained from the adsorption isotherms at different temperatures were used to calculate thermodynamic quantities such as ΔG^0, ΔH^0, and ΔS^0 of adsorption. The results indicate that dyes adsorption onto WNMC were feasible, spontaneous, and endothermic (37) in nature.

Breakthrough Capacity through Column Studies

In practice the column type continuous flow operations have distinct advantages over batch treatment. The sorption dose (1 gm) along the diameter (1 cm) was situated by introducing by concentrate variation (50 mg/l, 80 mg/l) of MG and CR solution as a rate of 1 ml/min. Samples were collected from ports after 50 ml. The results presented as the ratio to the effluent concentration (C/C_0) versus different time intervals (Fig. 7). Initially, the feed solution was in contact with the fresh adsorbent at the bottom of the column. The dyes were adsorbed progressively on the sorbent as it flowed upward. As more fluid is fed to the column, the bottom portion of the adsorbent becomes saturated with these dyes; thus, the adsorption zone moves upwards. Therefore, the concentration of the solute in the lower portion of the packed bed was usually higher than that in the top portions. The breakthrough capacity of the adsorbent for Malachite green has been calculated as 60.25 mg/g. As can be seen in Fig. 7, the breakthrough capacity of the adsorbent for Congo red has been calculated as 40 mg/g. For systems involving a spontaneous adsorption process, a straightforward approach may be adopted for the design of a fixed bed adsorber provided the rate of attainment of equilibrium of the solute concentration between the solution and the adsorbed phase is known (38).

BDST Model

The breakthrough data from the column studies can be described by the BDST model. The BDST model is based on physically measuring the capacity of the bed at different breakthrough values. This simplified design model ignores the intraparticle mass transfer resistance and external film resistance such that the adsorbate is adsorbed onto the adsorbent surface directly. With these assumptions, the BDST model works well and provides useful modeling equations for the changes of the system parameters. The lines of t vs. Z at values of C_t/C_0 (0.2, 0.4, and 0.6) are shown in (Fig. 8) respectively. The related constants of BDST according to the slopes and intercepts of the lines are listed in Table 5. The uncertainties of the relative parameters are also listed in Table 5. The adsorption capacity of the bed per unit bed volume, N_0, was calculated from the

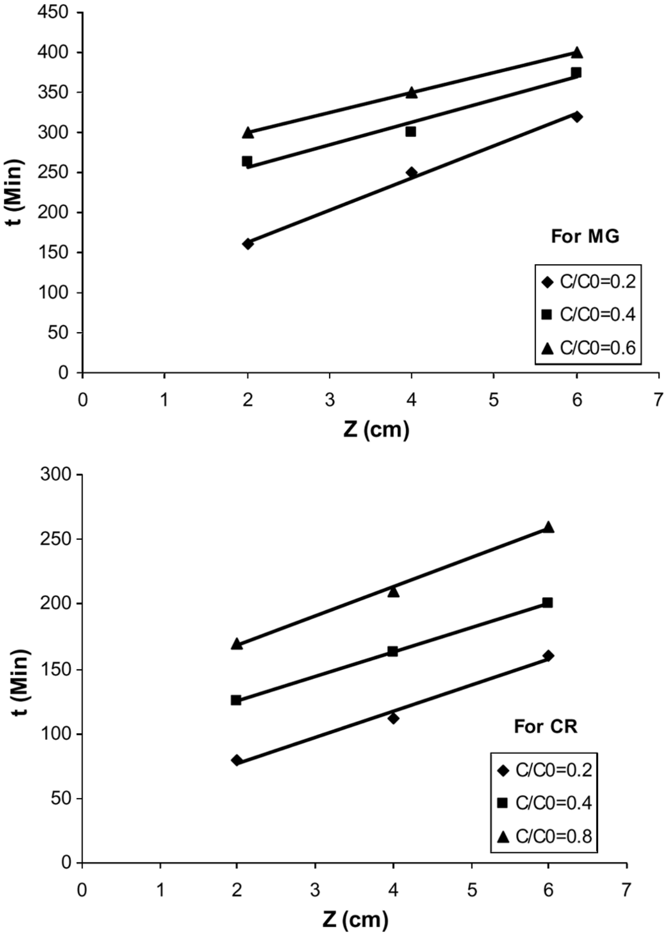

FIG. 8. Bed depth service time model of MG and CR.

TABLE 5
The calculated constants of BDST model for the adsorption of MG and CR ($C_0 = 10\,mg^{-1}$, $v = 1\,ml\,min^{-1}$)

	K_a		N_0		R^2	
C_t/C_0	MG	CR	MG	CR	MG	CR
0.2	−0.000554	−0.00123	3200	1600	0.994	0.986
0.4	−0.000067	−0.00018	2250	1500	0.964	0.999
0.6	−0.000068	−0.00021	2000	1800	0.992	0.995

slope of BDST plot, assuming initial concentration, C_0, and linear velocity, υ, as constant during the column operation. The rate constant, K_a, calculated from the intercept of BDST plot, characterizes the rate of solute transfer from the fluid phase to the solid phase (39). With the values of C_t/C_0 increasing, the values of N_0 increased while K_a decreased. The BDST model parameters can be helpful to scale up the process for other flow rates without further experimental run.

Desorption Studies

Desorption studies help to elucidate the nature of adsorption recycling of the spent adsorbent and the dye. If the adsorbed dye can be desorbed using neutral pH water, then the attachment of the dye on the adsorbent is by weak bonds. If sulphuric acid or alkaline water can desorb the dye, then the adsorption is by ion exchange. If an organic acid, like acetic acid can desorbs the dye, then the dye is held by the adsorbent through chemisorptions. Sodium hydroxide and sulphuric acid (1 M) did not show any desorption but weak acid, like acetic acid (5 M) solubilized about 86.24% of MG and 72.45% of CR from the spent adsorbent (Fig. 9). Desorption of the dye in acetic acid indicates that dyes are adsorbed onto WNMC through chemisorptions mechanism and very little desorption of dye in acid or base confirms the strong affinity of the dye on the WNMC.

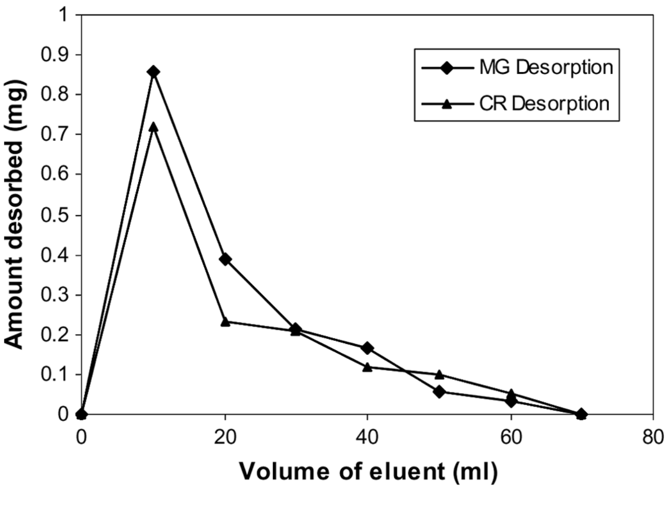

FIG. 9. Regeneration of spent adsorbent (Flow rate – 1 ml/min, dose – 1 g, dia – 1 cm, temperature – 30 ± 5°C).

CONCLUSION

1. The SEM and FTIR analysis revealed that the activation influenced the surface chemistry of the water nut shell.
2. Thermodynamic parameter such as the entropy (0.1766 $kj\,mol^{-1}$, 0.1403 $kj\,mol^{-1}$), enthalpy change (48.970 $kj\,mol^{-1}$, 42.191 $kj\,mol^{-1}$) and standard free energy are also determined, and the results shows that the adsorption process was found to be feasible, endothermic, and spontaneous.
3. The mechanism of adsorption was found to conform to the pseudo-second-order kinetics and follows the Langmuir model with a good correlation.
4. The use of BDST model in this way provides a realistic description of the adsorption of MG and CR by WNMC and the empirical data can be adopted in predicting the bed depth or service time for a specified set of influent characteristics for the scale-up of the sorption column. An increase in bed height resulted in improved sorption performance. The BDST model constants were determined and proposed for use in column design.
5. Overall, WNMC shows excellent adsorptive characteristics for the removal of dyes and appears as a very promising sorbent due to its high uptake capacity and to its low cost.

ACKNOWLEDGEMENTS

The authors are thankful to the chairman, Department of Applied Chemistry, Aligarh Muslim University, Aligarh (India) for providing research facilities and also thankful to the UGC (University Grants Commission) for providing financial assistance to one of the authors, Pijush Kanti Mondal.

REFERENCES

1. McKay, G.; Allen, S.J.; McConvey, I.F.; Otterburn, M.S. (1981) Transport process in the sorption of colored ions by peat particles. *Journal of Colloid and Interface Science*, 80 (2): 323–339.
2. Suryadi, I.; Bhatia, S.K. (2000) Adsorption of flavor esters on granular activated carbon. *Canadian Journal of Chemical Engineering*, 78: 892–901.
3. Ahmad, R.; Mondal, P.K. (2009) Application of acid treated almond peel for removal and recovery of brilliant green from industrial wastewater by column operation. *Separation Science and Technology*, 44: 1638–1655.
4. Hsueh, C.L.; Huang, Y.H.; Wang, C.C.; Chen, S. (2005) Degradation of azo dyes using low iron concentration of Fenton and Fenton-like system. *Chemosphere*, 58: 1409–1414.

5. Muruganandham, M.; Swaminathan, M. (2004) Decolourisation of reactive orange 4 by Fenton's and photo Fenton oxidation technology. *Dyes & Pigments*, 63: 315–321.
6. Houas, A.; Lachheb, H.; Ksibi, M.; Elaloui, E.; Guillard, C.; Herrmann, J.M. (2001) Photocatalytic degradation pathway of methylene blue in water. *Appl. Catal. B: Environ.*, 31: 145–157.
7. Ao, C.H.; Lee, S.C. (2004) Combination effect of activated carbon with TiO_2 for the photodegradation of binary pollutants at typical indoor air level. *J. Photochem. Photobiol A*, 161: 131–140.
8. Robinson, T.; Chandran, B.; Nigam, P. (2001) Studies on the production of enzymes by white-rot fungi for the decolorization of textile dyes. *Enzyme Microb. Technol*, 29: 575–579.
9. Park, C.; Lee, Y.; Kim, T.-H.; Lee, B.; Lee, J.; Kim, S. (2004) Decolorization of three acid dyes by enzymes from fungal strains. *J. Microbiol. Biotechnol.*, 14: 1190–1195.
10. Namasivayam, C.; Kavitha, D. (2002) Removal of Congo red from water by adsorption onto activated carbon prepared from coir pith, an agricultural solid waste. *Dyes & Pigments*, 54: 47–58.
11. Nagarethinam, K.; Mariappan, M. (2002) Adsorption of Congo red on various activated carbons. *Water Air Soil Pollution*, 138: 289–305.
12. Fierro, V.; Torné-Fernández, V.; Montané, D.; Celzard, A. (2008) Adsorption of phenol onto activated carbons having different textural and surface properties. *Microporous Mesoporous Materials*, 111 (1–3): 276–284.
13. Girgis, B.S.; El-Hendawy, A.A. (2002) Porosity development in activated carbon obtained from date pits under chemical activation with phosphoric acid. *Microporous Mesoporous Mater*, 52: 105–117.
14. Girgis, B.S.; Khalil, L.B.; Tawfik, T.A.M. (2000) Porosity characteristics of activated carbons from olive wastes impregnated with H_3PO_4. *Adsorption Sci. Tech.*, 18 (4): 373–83.
15. Philip, C.A.; Girgis, B.S. (1996) Adsorption characteristics of microporous carbons from apricot stones activated by phosphoric acid. *J Chem. Technol. Biotechnol.*, 67: 248–254.
16. Mohan, D.; Singh, K.P.; Sinha, S.; Ghosh, D. (2004) Removal of pyridine from aqueous solutions using low-cost activated carbons derived from agricultural waste materials. *Carbon*, 42: 2409–2421.
17. Goel, J.; Kadirvelu, K.; Rajagopal, C.; Garg, V.K. (2005) Removal of lead(II) by adsorption using treated granular activated carbon: Batch and column studies. *J. Hazard. Mater.*, 125: 211–220.
18. Ko, D.C.K.; Porter, J.F.; McKay, G. (2000) Optimised correlations for the fixed-bed adsorption of metal ions on bone char. *Chem. Engg. Sci.*, 55: 5819–5829.
19. Othman, M.Z.; Roddick, F.A.; Snow, R. (2001) Removal of dissolved organic compounds in fixed-bed columns: Evaluation of low-rank coal adsorbents. *Water Res.*, 35: 2943–2949.
20. Tan, I.A.W.; Ahmad, A.L.; Hameed, B.H. (2008) Enhancement of basic dye adsorption uptake from aqueous solutions using chemically modified oil palm shell activated carbon. *Colloid and Surfaces A*, 318: 88–96.
21. Ho, Y.S. (2004) Citation review of lagergren kinetic rate equation on adsorption reactions. *Scientometrics*, 59 (1): 171–177.
22. Ho, Y.S.; McKay, G. (1998) Sorption of dye from aqueous solution by peat. *Chem. Engineering Journal*, 70 (2): 115–124.
23. Ho, Y.S.; McKay, G. (1999) Pseudo-second order model for sorption processes. *Process Biochemistry*, 34 (5): 451–465.
24. Ho, Y.S.; McKay, G. (2000) The kinetics of sorption of divalent metal ions onto sphagnum moss peat. *Water Research*, 34: 735–742.
25. Ho, Y.S.; McKay, G. (1998) The kinetics of sorption of basic dyes from aqueous solutions by sphagnum moss peat. *Canadian Journal of Chemical Engineering*, 76: 822–826.
26. Kuo, S.; Lotse, E.G. (1973) Kinetics of phosphate adsorption and desorption by hematite and gibbsite. *Soil Science Society Am. Journal*, 116: 400–406.
27. Ayyappan, R.; Carmalin Sophia, A.; Swaminathan, K.; Sandhya, S. (2005) Removal of Pb(II) from aqueous solution using carbon derived from agricultural wastes. *Process Biochem.*, 40: 1293–1299.
28. Weber, Jr. W.J.; Morris, J.C.; Saint, J. (1963) Kinetics of sorption of carbon from solution. *Engineering Div. Am. Soc. Civil Eng.*, 89: SA2–SA31.
29. Arslano glu, F.N.; Kar, F.; Arslan, N. (2005) Adsorption of dark coloured compounds from peach pulp by using granular activated carbon. *J. Food Engg.*, 68: 409–417.
30. Langmuir, I. (1918) The adsorption of gases on plane surfaces of glass, mica and platinum. *Journal of American Chem. Soc*, 40: 1361.
31. Weber, T.W.; Chakkravorti, R.K. (1974) Pore and solid diffusion models for fixed-bed Adsorbers. *AlChE J.*, 20: 228.
32. Freundlich, H.M.F. (1906) Over the adsorption in solution. *J. Phys. Chem.*, 57: 385–470.
33. Haghseresht, F.; Lu, G. (1998) Adsorption characteristics of phenolic compounds onto coal-reject-derived adsorbents. *Energy Fuels*, 12: 1100–1107.
34. Fytianos, K.; Voudrias, E.; Kokkalis, E. (2000) Sorption-desorption behavior of 2,4-dichloriphenol by marine sediments. *Chemosphere*, 40: 3–6.
35. Namasivayam, C.; Prabha, D.; Kumutha, M. (1998) Removal of direct red and acid brilliant blue by adsorption on to banana pith. *Bioresource Technology*, 64: 77–79.
36. Dogan, M.; Alkan, M.; Turkyılmaz, A.; Ozdemir, Y. (2004) Kinetics and mechanism of removal of methylene blue by adsorption onto perlite. *Journal of Hazardous Material*, 109: 141–148.
37. Ozcan, A.; Oncu, E.M.; Ozcan, A.S. (2006) Adsorption of Acid Blue 193 from aqueous solutions onto DEDMA-sepiolite. *Journal of Hazardous Materials*, 129: 1–3.
38. Weber, Jr. W.J. (1972) Physicochemical Process for Water quality Control. New York: *Wiley-Interscience*.
39. Padmesh, T.V.N.; Vijayaraghavan, K.; Sekaran, G.; Velan, M. (2005) Batch and column studies on biosorption of acid dye on fresh water macro alga Azolla filiculoides. *Journal of Hazardous Material*, 125: 121–129.